GFZ
Helmholtz-Zentrum
POTSDAM

Originally published as:

Comina, C., Krawczyk, C. M., Polom, U., Socco, L. V. (2017): Integration of SH seismic reflection and Love-wave dispersion data for shear wave velocity determination over quick clays. - *Geophysical Journal International*, *210*, 3, pp. 1922—1931.

DOI: http://doi.org/10.1093/gji/ggx276

Geophysical Journal International

Geophys. J. Int. (2017) **210,** 1922–1931
Advance Access publication 2017 June 26
GJI Marine geosciences and applied geophysics

doi: 10.1093/gji/ggx276

Integration of *SH* seismic reflection and Love-wave dispersion data for shear wave velocity determination over quick clays

Cesare Comina,[1] Charlotte M. Krawczyk,[2,3] Ulrich Polom[4] and Laura Valentina Socco[5]

[1]*Department of Earth Sciences (DST), Università degli Studi di Torino, via Valperga Caluso* 35, *I*-10125, *Italy. E-mail: cesare.comina@unito.it*
[2]*GFZ German Research Centre for Geosciences, Telegrafenberg, D*-14473 *Potsdam, Germany*
[3]*Technische Universität Berlin, Ernst-Reuter-Platz* 1, *D*-10587 *Berlin, Germany*
[4]*Leibniz Institute for Applied Geophysics, Stilleweg* 2, *D*-30655 *Hannover, Germany*
[5]*Department of Environment, Land and Infrastructure Engineering (DIATI), Politecnico di Torino, corso Duca degli Abruzzi* 24, *I*-10129, *Italy*

Accepted 2017 June 23. Received 2017 June 21; in original form 2017 January 20

SUMMARY

Quick clay is a water-saturated formation originally formed through flocculation and deposition in a marine to brackish environment. It is subsequently leached to low salinity by freshwater flow. If its strength decreases, then the flocculated structure collapses leading to landslides of varying destructiveness. Leaching can result in a reduction of the undisturbed shear strength of these clays and suggestions exist that a reduction in shear wave velocities is also possible. Integration of *SH* seismic reflection and Love-wave dispersion data was undertaken, in an area near the Göta River in southwest Sweden, to evaluate the potential of shear wave velocity imaging for detecting quick clays. Seismic reflection processing evidenced several geologically interesting interfaces related to the probable presence of quick clays (locally confirmed by boreholes) and sand-gravelly layers strongly contributing to water circulation within them. Dispersion data were extracted with a Gaussian windowing approach and inverted with a laterally constrained inversion using *a priori* information from the seismic reflection imaging. The inversion of dispersion curves has evidenced the presence of a low velocity layer (lvl, with a velocity reduction of *ca.* 30 per cent) probably associable to quick clays. This velocity reduction is enough to produce detectable phase-velocity differences in the field data and to achieve a better velocity resolution if compared to reflection seismic velocity analyses. The proposed approach has the potential of a comprehensive determination of the shear wave velocity distribution in the shallow subsurface. A sensitivity analysis of Love-wave dispersion data is also presented underlining that, despite limited dispersion of the data set and the velocity-reducing effect of quick-clay leaching, the proposed interpretation procedure arises as a valuable approach in quick clay and other lvl identification.

Key words: Inverse theory; Acoustic properties; Surface waves and free oscillations.

1 INTRODUCTION

Quick clays are worldwide spread, particularly in Nordic countries (Torrance 1983; Rankka *et al.* 2004) and Canada (Crawford 1968; Choquette *et al.* 1987), causing several landslides of varying size and destructiveness (Geertsema *et al.* 2006; Lundström *et al.* 2009). Quick clay is a water-saturated clay composed of saline silts and clays deposited in a marine to brackish environment. If these clays are uplifted above sea level, they can be leached to low salinity by freshwater flow. The decrease of salt content, which originally contributed to the bonding between clay particles, could cause a strength reduction (Osterman 1964; Choquette *et al.* 1987), causing, as extreme, the collapse of the flocculated structure and the liquefaction of quick clay. It is, therefore, of major importance to detect the presence of quick clays and determine their associated risk of failure.

In many sites, boreholes showed that flocculated material overlies coarse-grained units: glaciofluvial sands formed at the end of deglaciation, when the sea level was high relative to the local land level (Malehmir *et al.* 2013). These permeable units are a potential path for freshwater intrusion causing an acceleration in the naturally slow salt leaching process and quick-clay formation with later destabilization.

From the geotechnical point of view, a clay is defined ‘quick’ when its sensitivity (the ratio of undrained shear strength in undisturbed conditions and undrained remoulded shear strength) is above 30 and its remolded shear strength is less than 0.5 kPa (Torrance 1983). Quick-clay identification using geotechnical field and laboratory testing can be carried out based on these parameters. However, geotechnical testing is often sparse and lack correlation among wider investigation areas. Geophysical methods can be used alternatively to distinguish quick-clay formations using the variations in

© The Authors 2017. Published by Oxford University Press on behalf of The Royal Astronomical Society.

geophysical parameters (e.g. resistivity and seismic velocities) as a proxy for quick-clays geotechnical properties. Geophysical methods offer the advantage to bridge the gaps between geotechnical information over wider areas.

Seismic and electrical resistivity methods are particularly useful for geophysical characterization of quick clays (e.g. Malehmir *et al.* 2013). So far, mostly electrical methods have been used. Field studies compared electrical resistivity values and salt content (Söderblom 1969; Solberg *et al.* 2008) to detect the presence of leached formations. Unleached marine clay, which contains a larger concentration of ions in its pore water, shows usually low values (below 10 Ω·m) of resistivity. For quick clay, where significant leaching of salt has occurred, the resistivity values are usually higher. Different resistivity ranges have been proposed in literature (Solberg *et al.* 2008; Dahlin *et al.* 2013; Sauvin *et al.* 2013).

The seismic wave velocity, particularly shear wave velocity (*Vs*), which depends on the mechanical properties of the soil skeleton only, is also a potentially useful geophysical parameter. First, among several, Bjerrum (1954) showed that leaching can result in a reduction of the undisturbed shear strength of marine clay due to the reduced bonding between clay particles. This leads to the fact that the shear strength, together with resistivity, can also vary with reduced salt concentration. This was confirmed by the analysis of a number of landslides occurring without external causes and by laboratory data (Bjerrum 1954). Empirical correlations between *Vs* and undrained shear strength determined in triaxial or direct shear tests and with empirical interpretations of geotechnical *in situ* testing have been established (Dickenson 1994; Andersen 2004; Taboada *et al.* 2013). Specific correlations have also been proposed for Norwegian clays (NGI 2015; L'Heureux & Long 2017). Even if their general quantitative validity is debated, most of these correlations report an exponential reduction in *Vs* following a reduction in the undrained shear strength. Therefore, shear wave seismic methods could potentially be an alternative approach, with respect to the more established resistivity-based methods, for locating and mapping quick-clay formations. This is particularly true if the investigated formations are near their stability limit (i.e. undergoing a significant shear strength reduction). Quick and non-quick clays can be therefore distinguished based on the evidence of shear wave velocity reduction related to the shear strength reduction. Moreover, given the above correlations, information about the shear resistance can be extracted from seismic data and used as first input for geotechnical modeling and stability assessment.

Yet, differences in *Vs* and shear resistance between flocculated and dispersed structures, evidenced by laboratory and geotechnical data, might not be large enough to produce seismic velocity variations that can be detected and interpreted in practice with geophysical field surveys. There is a lack of information published on the evidence of shear wave velocity reduction in presence of quick clays. Donohue *et al.* (2012) performed multichannel analysis of surface waves (MASW) over quick clays suggesting that further work is necessary to fully investigate the effect of leaching on *Vs* and that 2-D *Vs* profiles could be useful for improving site characterization in areas of quick clays. Sauvin *et al.* (2013) used the MASW method to recover shear wave velocities for quick-clay mapping along profiles. They concluded that the weak bonding of clay particles, that could potentially lead to a decrease of shear wave velocity and attenuation in leached clays, needs to be further investigated since no clear evidence has been found in the analysed data (Sauvin *et al.* 2013). Interesting results have been reported by Fabien-Ouellet *et al.* (2014) who showed that joint acquisition and processing of *SV* (vertically polarized shear waves) reflections and Rayleigh waves provided a more complete and accurate reconstruction of the velocity structure than the two methods taken separately. Authors also observed variations in shear wave velocities in the sensitive clays comparable to the results of SCPTu (Seismic Cone Penetration Test with pore pressure measurement).

Moreover mapping coarse-grained units related to the quick-clay presence is also of major importance for the definition of the risk associated to landslides. Seismic methods, and particularly high-resolution *SH* (horizontally polarized shear waves) seismic reflection, are more suitable for a detailed mapping of these ancillary formations with respect to resistivity-based methods, since they offer a better structural resolution of interfaces. Such structural identification of quick-clay layers has been successful for instance in Trondheim (Polom *et al.* 2010) or close to Gotenburg (Krawczyk *et al.* 2013a; Malehmir *et al.* 2013).

Seismic methods are, therefore, used in this paper to investigate both the presence of relevant interfaces related to gravelly layers and the effect of quick clay on shear wave velocity in field data. High-resolution *SH* reflection and Love-wave dispersion data extracted from the same data set were integrated to recover a comprehensive shear wave velocity model along a seismic line acquired over a potentially unstable quick-clay area.

2 TEST SITE

High-resolution *SH* reflection data have been acquired, along several profiles, as part of a joint project studying clay-related landslides in Nordic countries (Krawczyk *et al.* 2013a; Malehmir *et al.* 2013). The experimental site is in Fråstad, an area near the Göta River, north of the village Lilla Edet in southwest Sweden. The site is located (Löfroth *et al.* 2011) near a known landslide scar (Fig. 1) at

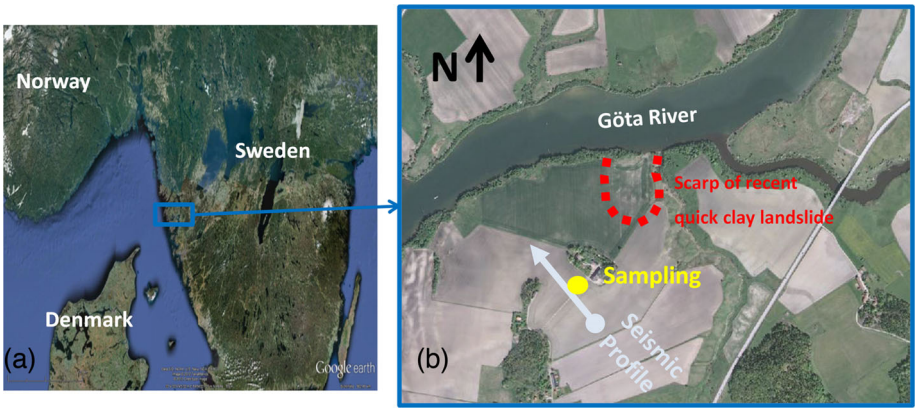

Figure 1. (a) Location of the study area, with details on the orientation of analysed seismic profile (grey) and (b) borehole (yellow).

an average height above sea level of about 25 m. Several other quick-clay-related landslides have been observed in the surroundings. On 1957 June 7, a disastrous quick-clay landslide affected an area of 32 ha, located several kilometres south of the test site, and hit the Göta community leaving three fatalities (Nadim *et al.* 2008). Göta River is the source of drinking water for about 700 000 people and is extensively used for industrial transportation. Therefore, areas near the river are highly industrialized and populated even though they are well known for several hazardous quick-clay landslides during the last century.

Geological reconstruction of the formations at the investigated site reported the presence of a mixture of silty clay to clayey silt and sandy silt which were originally deposited in a marine to brackish environment (Lundström *et al.* 2009; Solberg *et al.* 2012). After deglaciation, these marine sediments were uplifted above sea level and leached to low salinity by fresh water intrusion. This formation process reflects the potential presence of quick clays in the area, which may lead to rapid liquefaction, in most cases triggered by an external initial force (e.g. intense rainfalls).

Geotechnical surveys on site (CPT, Cone Penetration Tests, and CPTu, Cone Penetration Tests with pore pressure measurement) and laboratory testing have been performed in the area. Results of these surveys suggested the presence of coarse-grained material at a depth range of 20–30 m. Interestingly, in most places quick clays were found to overlie this coarse-grained material. A detailed description of the geotechnical data can be found in Löfroth *et al.* (2011).

Local stratigraphy and sediment cores are available at the site from a borehole (Salas-Romero *et al.* 2016) that is located near the centre of the analysed shear wave reflection seismic profile (10 m apart from the profile plane; Fig. 1b). A simplified stratigraphic column from the borehole is reported in Fig. 3(a). Direct sounding and laboratory tests evidence, between 6 and 7 m depth, the presence of a clay formation with liquid limit about 65 per cent, natural water content about 71 per cent and sensitivity around 49 (SGI 2012), which is probably a quick-clay formation. Similar properties have also been noted in a deeper portion of the sounding, below a coarser sand–silt–gravel formation which separates these two quick-clay layers. The lower boundary of quick clay at about 15–20 m depth is in accordance with the surface elevation of the most recent landslide scar seen in the study area (Fig. 1b). Bedrock was reached at nearly 35 m depth (Salas-Romero *et al.* 2016).

3 SEISMIC REFLECTION DATA

The data analysed in this work refer to a single high-resolution *SH* seismic line acquired over the soft sediments of a stubble field (for location, see Fig. 1). This specific data set has been selected, among several acquired lines, because of the presence of weak Love waves, showing dispersive pattern. Acquisition was performed by means of a land streamer consisting of 120 (10 Hz) horizontal geophones perpendicular to the survey line at 1 m spacing. A source sweep signal of 20–160 Hz, 10 s duration, was emitted every 2 m along the profile by an ELVIS - Electrodynamic Vibrator System (e.g. Polom *et al.* 2008; Krawczyk *et al.* 2012). Two different spreads were used during the data acquisition for a total survey length of about 250 m. Example shot gathers (following pre-processing) are reported in Fig. 2 with evidence of both shallow and deep reflections and dispersive Love waves.

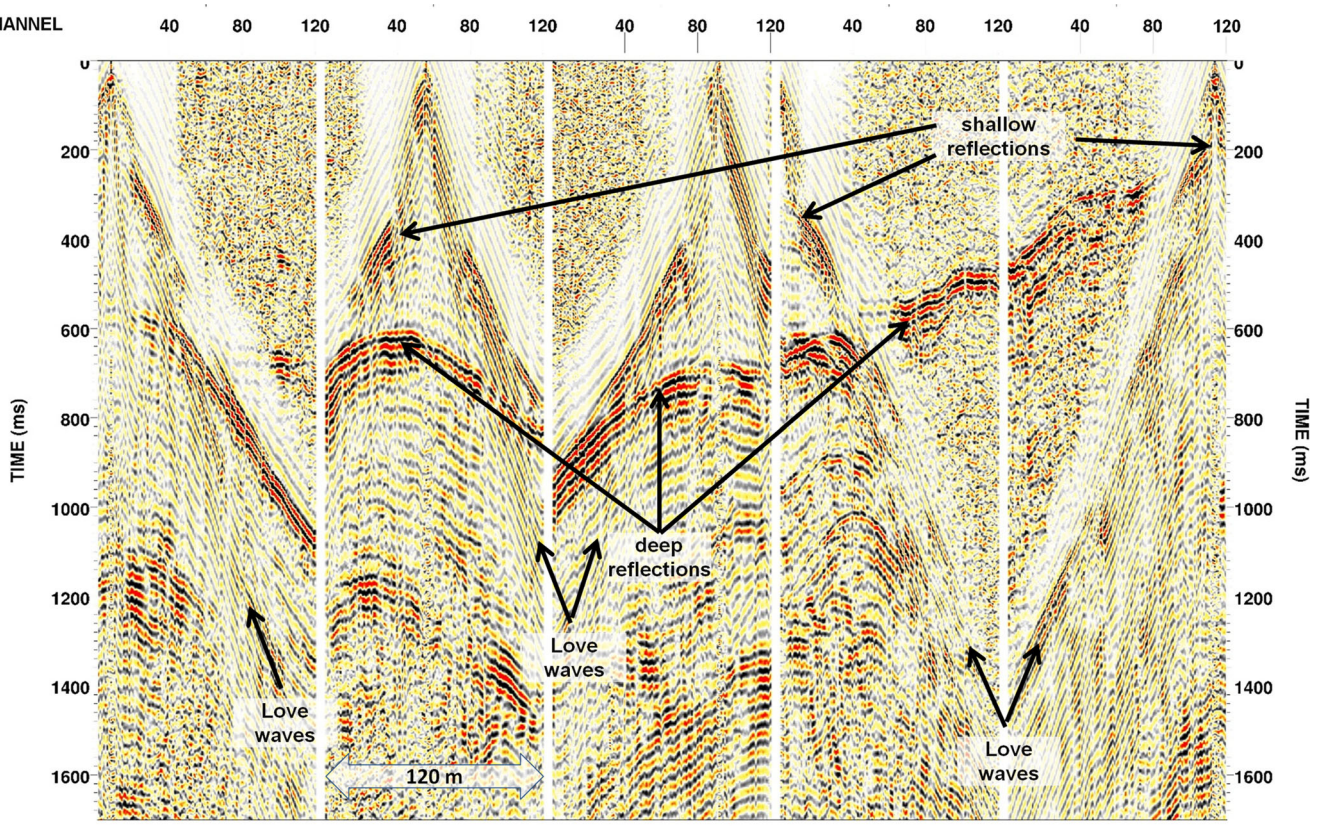

Figure 2. Example shot gathers (following pre-processing) from the reflection survey with evidence of both shallow and deep reflections and dispersive Love waves.

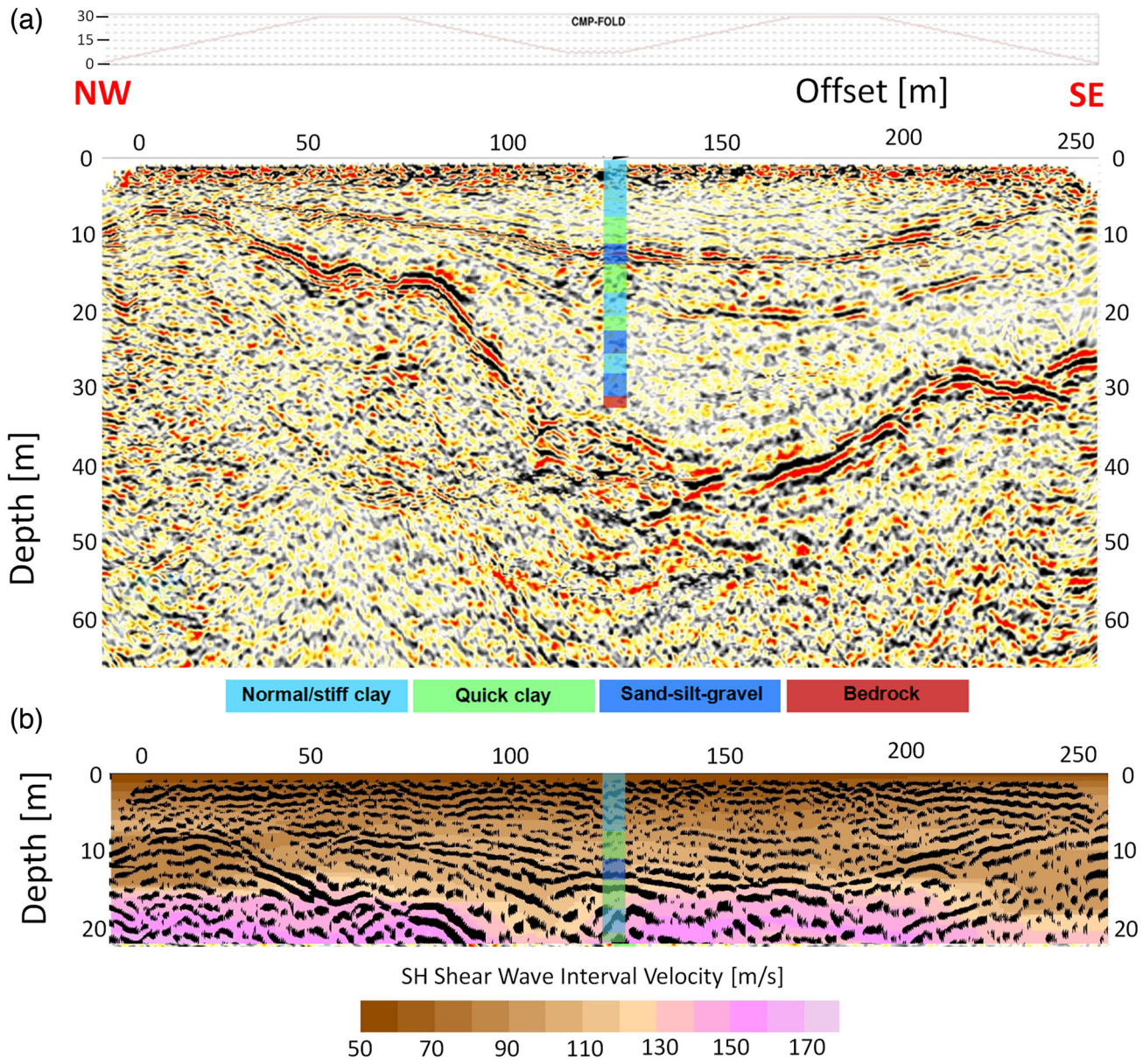

Figure 3. Time-to-depth converted, FD-migrated seismic section along the surveyed line (a) with simplified lithologic stratigraphy from the borehole (vertical bar in the middle; lithology from Salas-Romero *et al*. 2016) superimposed and the *S*-wave interval velocity field derived from velocity analysis from seismic reflection data for the first 20 m of the section (b).

After quality control, correlation, subtractive stack and geometry setup, the subsequent main processing procedure of the *SH*-wave seismic data encompassed amplitude scaling, bandpass filtering, *f*–*k* filter, common midpoint (CMP) sorting, velocity analysis, normal moveout correction, CMP stacking, predictive deconvolution, finite-difference (FD) migration and time-to-depth conversion.

The migrated depth section (after Polom *et al.* 2013), combined with the evidence from the borehole, is reported in Fig. 3(a). Fig. 3(b) presents the first 20 m of the seismic reflection profile superimposed on the interval velocities derived from the velocity analysis of the seismic data. Interval velocities were retrieved only for the top portion of the surveyed line due to the absence of strong reliable reflectors at depth. The structural inventory is imaged down to *ca.* 50 m depth with a vertical resolution of at least 1 m. The minimum vertical resolution is nearly 30 cm in the sand–silt–gravel layer at 8 m depth at offset 80 m.

In the seismic section, the top of the basement, with a rough bowl-shaped topography mildly dipping from NW to SE, is clearly evident. Horizontally layered sediments overlying the bedrock are also visible in the upper 20 m depth of the section.

A slight mismatch with the borehole evidence, of nearly 3 m, for the bedrock depth detection is observed in the middle of the profile. One reason for this mismatch may be the low CMP fold at this location. However, 3-D effects, caused by the irregular bowl-shaped bedrock topography projected into the 2-D section, and the offline offset of the borehole are more likely responsible for the depth difference.

One can note three distinct sediment sequences (units) delineated by high-amplitude reflectors above the bedrock (Figs 3a and 7a). The shallowest seismic reflectors exhibits characteristics similar to the ones observed on *P*-wave data gathered in close vicinity (Malehmir *et al.* 2013), implying that it may originate from a coarse-grained

layer, as also confirmed by direct sounding evidence. This layer, mostly responsible of water circulation, leads to an acceleration in leaching of the clays above and below it and to quick-clays formation. The topography of this reflector and the bedrock topography were picked along the seismic line and used as *a priori* information during the inversion of Love-wave dispersion curves.

Comparison of the simplified stratigraphic column (Salas-Romero *et al.* 2016) with the seismically derived velocity field (Fig. 3b) shows no clear velocity indication to distinguish between quick-clay and stiff-clay layers. This is probably caused by the small velocity contrast of these units and the long aperture of more than −25 m to +25 m offset range of the recording setup regarding depths below 12 m. Improving the aperture and, consequently, the velocity resolution in this very low velocity environment, would require smaller geophone and source intervals (e.g. below 0.5 m instead of the actual spacing of 1 m). Due to the lack of strong reflectors below the bedrock, a reliable analysis of the bedrock interval velocity could not be achieved. Therefore, the obtained bedrock velocity, resulting from the continuation of the rms velocity trend from above bedrock, is too low with respect to the expected bedrock velocity.

4 PROCESSING AND INVERSION OF LOVE-WAVE DATA

Several Love-wave dispersion curves are extracted from the same seismic records used for reflection interpretation to obtain a 2-D shear wave velocity image. Because of relevant subsurface lateral variations, the dispersion curve extraction along the profile requires an approach able to optimize the lateral resolution. A Gaussian windowing approach suggested by Bergamo *et al*. (2012) was adopted for this purpose. The seismic line is spanned with a moving Gaussian window and dispersion curves are extracted at distinct positions in *f*–*k* domain.

For the present data set, after a preliminary design and several tests on the windowing parameters, the processing provided a set of eight evenly spaced dispersion curves along each of the two different spreads used during data acquisition. This corresponds to approximately a dispersion curve every 12 m along the two spreads (Fig. 4). The dispersion curves have been obtained within each window using an *f*–*k* transform of the raw data and stacking the spectra of several shots. An automatic maxima picking is carried out inside a pre-selected area of high amplitude in the stacked spectra. Uncertainties in the picking are evaluated taking into account the picking variability of different shots and is later used for inversion (see later Fig. 6). The fundamental mode is dominant in most of the *f*–*k* spectra. Given the relatively high-frequency sweep adopted in data acquisition (20–160 Hz), the spectra resulted to be noisy in the low-frequency band (i.e. below nearly 15 Hz—see later Figs 6 and 8a). The picking was however continued also in the noisy part of the spectra, when possible, but this strongly compromises the maximum depth of investigation and increases the experimental uncertainty at low frequencies (see later Fig. 6).

Fig. 5 shows the same dispersion curves given in Fig. 4, but in form of a pseudo-section where pseudo-depth corresponds to wavelength divided by 2.5 and colour-coded to phase velocity. These data are compared to the main reflectors interpreted from seismic reflection and the simplified stratigraphic column of direct sounding. The investigation depth of surface wave dispersion curves is limited, overall to *ca.* 12 m: this is a result the low seismic velocity of the sediments and high-frequency band of the sources that produce relatively small wavelengths. A lateral variability can be observed along the survey line in the low-frequency band that corresponds to larger depths. Coherently with interfaces imaged in the reflection data, the velocity increases abruptly with depth in the NW portion of the line (at least for some of the imaged dispersion curves) due to the arising bedrock (Fig. 4). This notable increase reveals a higher sensitivity of dispersion data compared to reflection velocity analysis with respect to the bedrock velocity identification (also due to the lack of coherent reflectors within the bedrock).

The obtained Love-wave dispersion curves were inverted using a laterally constrained inversion (LCI) scheme based on a pseudo-2-D model parametrization together with 1-D forward data simulation. Auken & Christiansen (2004) first introduced the LCI approach for the interpretation of resistivity data, and Wisén & Christiansen (2005) and Socco *et al*. (2009) successfully applied it for inversion of surface wave data. LCI is a deterministic inversion in which each 1-D model is linked to its neighbours with mutual constraints to provide a single pseudo-2-D model. *A priori* information extracted from the reflection section was used to define the position of the main interfaces and to impose the lateral continuity of some layers.

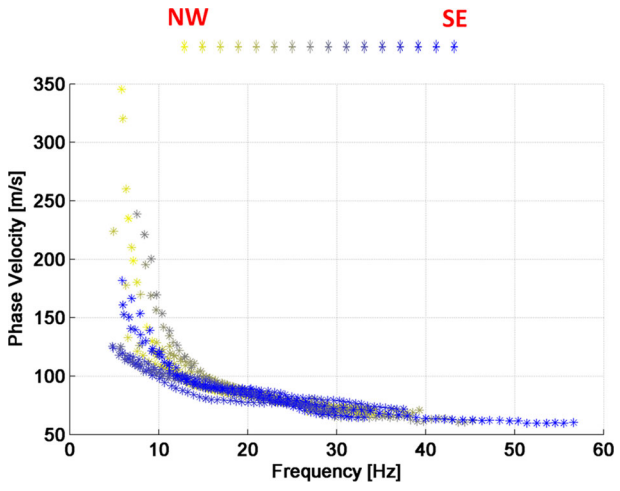

Figure 4. Dispersion curves extracted along the profile analysed with the moving Gaussian window approach; dispersion curves are coloured from yellow to blue from NW to SE.

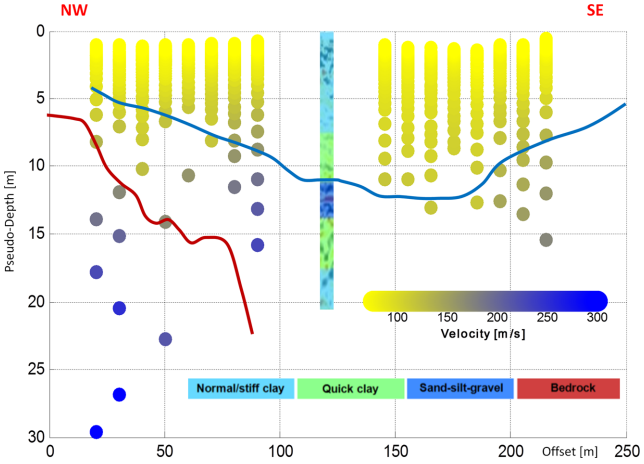

Figure 5. Dispersion curves extracted along the reflection seismic profile represented at the corresponding Gaussian window centers in terms of pseudo-depth (wavelength divided by 2.5) and colour-coded to phase velocity with simplified stratigraphic column from the borehole (vertical bar in the middle) and corresponding interfaces from seismic reflection data.

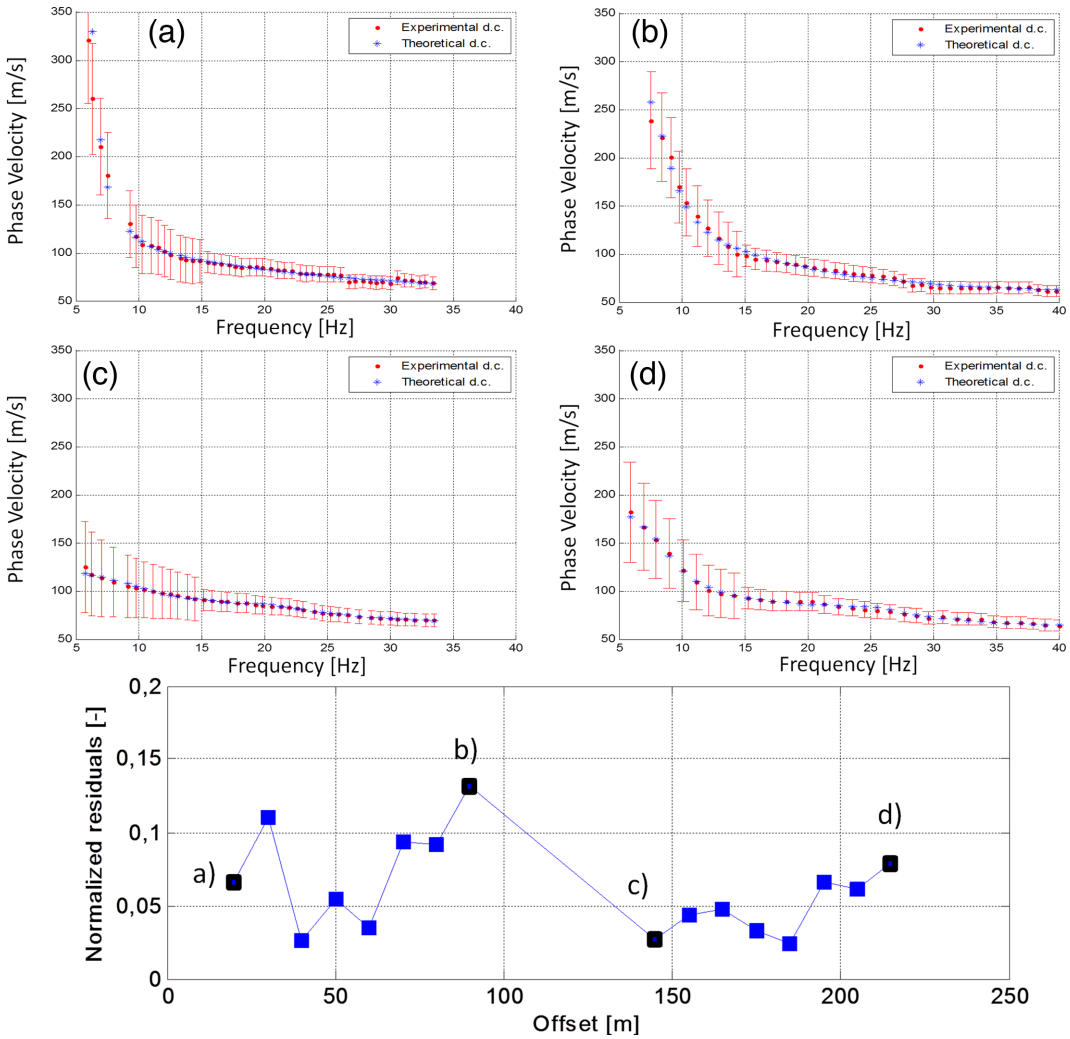

Figure 6. Normalized residuals of LCI along the profile (bottom) and some example fitting of experimental dispersion curves from (a) to (d).

Table 1. Adopted parametrization for LCI and lateral constraints.

Layer number	Initial shear wave velocity (m s^{-1})	Lateral constraint (m s^{-1})	Initial depth (m)	Lateral constraint (m)
1	60	5	1	2
2	120	–	6	–
3	250 (100 from 75 m offset)	–	From *SH* reflection	2
4	300	10	15 (from *SH* reflection before 75 m offset)	2
5	500 (300 from 75 m offset)	–		

Given the limited investigation depth, inversion was conducted to characterize the upper quick-clay layer.

A five-layer parametrization was adopted for LCI (Table 1). The first layer of the model is the shallower portion of the profile constituted by low velocity altered material, while the second layer is a progressively more compacted one. For both of these layers, no constraints on their initial values have been introduced in the inversion, but a strong constraint to ensure lateral continuity of the shallow layer has been introduced. The strength of the constraints are ruled by the value of the covariance (the lower the covariance, the stronger the constraint) which represents the expected lateral variability of the model parameters at the site (Table 1). *A priori* constraints have been instead imposed on the seismic interfaces imaged by seismic reflection: the bedrock surface in the NW portion and the coarser layer along the whole section (respectively, red and blue interfaces in Figs 5 and 7a). Hence, the depths of these interfaces are fixed in the inversion. Given the layered structure of the geological setting, we also imposed strong lateral constraints on the velocity of the sand–silt–gravel layer (which is imaged along the whole section) to ensure its continuity and lateral smoothness. No lateral constraints are instead imposed for the depth of the top of bedrock (which, given the limited investigation depth, is observable only in the NW portion of the line). A starting model with a slight velocity inversion (of 20 m s^{-1} from the above layer) at layer 3, which is supposed to be the quick-clay layer above the sand–silt–gravel interface, was adopted. Starting model velocities above the bedrock have been established following both reflection seismic velocity analysis and pseudo-depth representation.

Normalized residuals obtained at LCI inversion last iteration along the profile are reported in Fig. 6 together with some examples

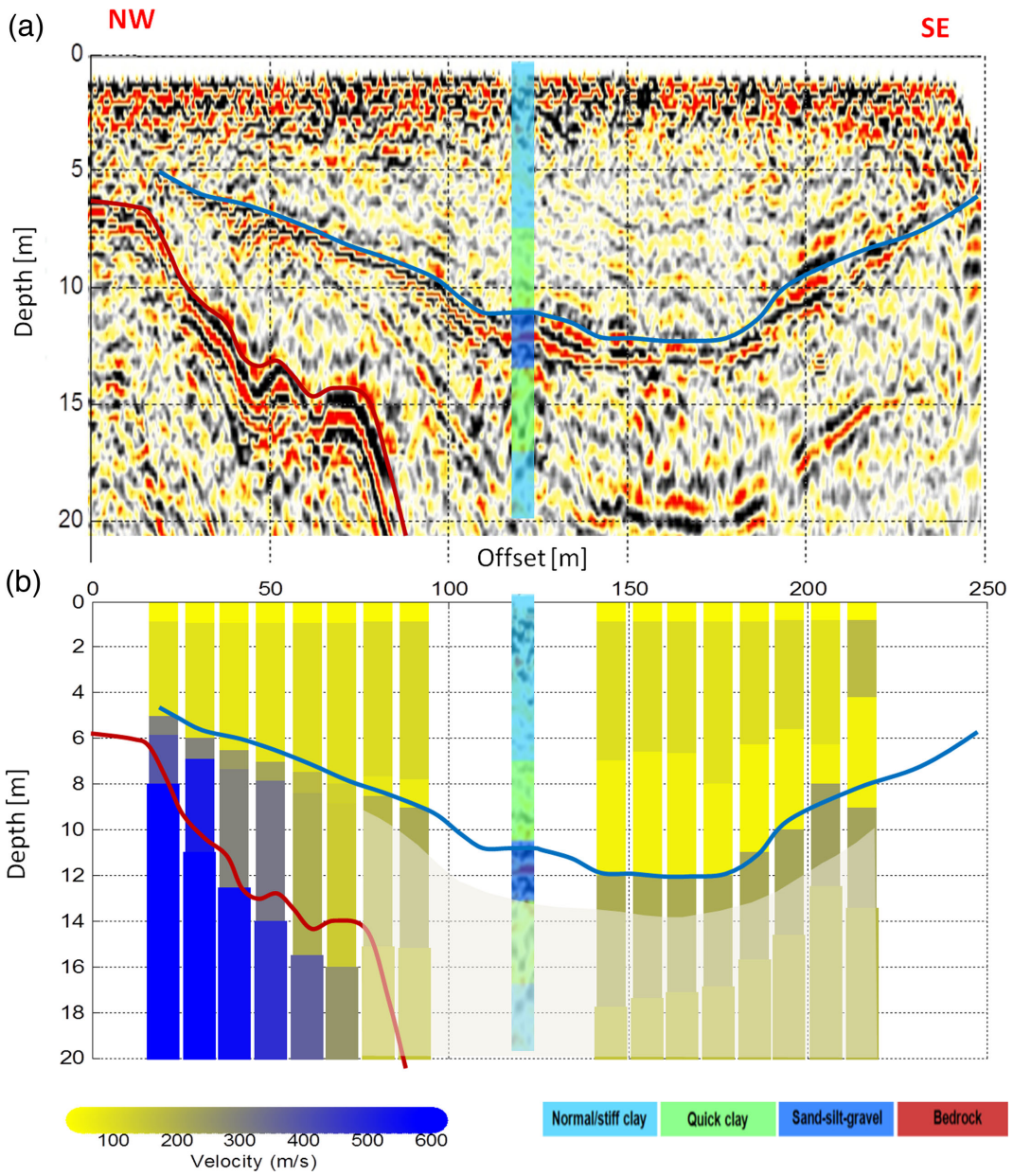

Figure 7. (a) Top part of the *SH* reflection section and (b) LCI inversion of the data set. Both images provide evidence of the main seismic interfaces and correlate with the stratigraphic column from borehole information.

of fitting between experimental and modeled dispersion curves. Dispersion curves fitting are particularly good for frequencies higher than 15 Hz where experimental uncertainties are lower. The average residual along the line is 6 per cent. Local higher residuals can be observed particularly near progressive 75 m (Fig. 6b), where the bedrock dips at the limit of the available investigation depth and this results in a higher lateral variability.

5 RESULTS AND DISCUSSION

Results of the LCI inversion of dispersion data are presented together with the reflection seismic image in Fig. 7. In Fig. 7(b), the shaded area (from 75 to 225 m offset) refers to the zone of the profile where the reliability of the inversion is reduced due to the limited penetration of dispersion data (see Fig. 5).

The final *S*-wave velocity model presents a low velocity layer (lvl), that is, the quick-clay layer, in the SE part of the section, which is locally comparable with the evidence from the direct sounding. The thickness of this layer is variable from SE to NW; as can be observed in Fig. 7(a), a weak but continuous reflection is imaged in the seismic section at this interface, most probably due to a low-impedance contrast. Indeed, considering the obtained velocity values and a constant density, the reflection coefficient at the faint reflection marking top of the quick clay layer can be estimated to approximately −0.22. The obtained velocity model also correctly depicts a higher velocity layer, comparable with the coarser sand–silt–gravel formation evidenced in the sounding and in seismic reflection data. This bright reflection at *ca.* 12 m depth has a reflection coefficient value of 0.53. The velocity model also gives clear evidence of the presence of the shallower bedrock in the NW portion of the line. Moreover, this analysis yields the bedrock velocity

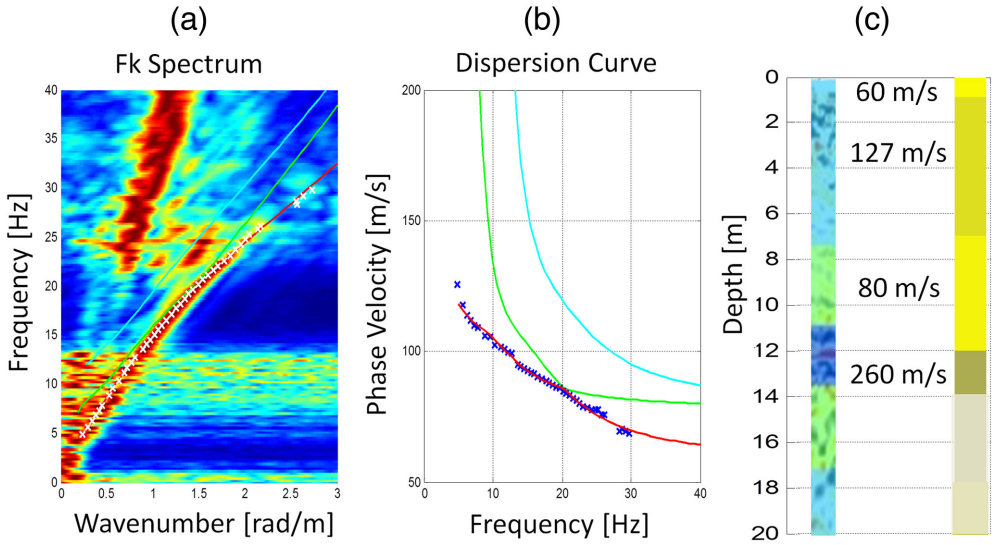

Figure 8. Forward multimodal modeling of a retrieved dispersion curve: first three modes plotted above (a) the picked dispersion curve and *f–k* spectrum, (b) velocity versus frequency data and (c) borehole lithology and shear wave velocity model.

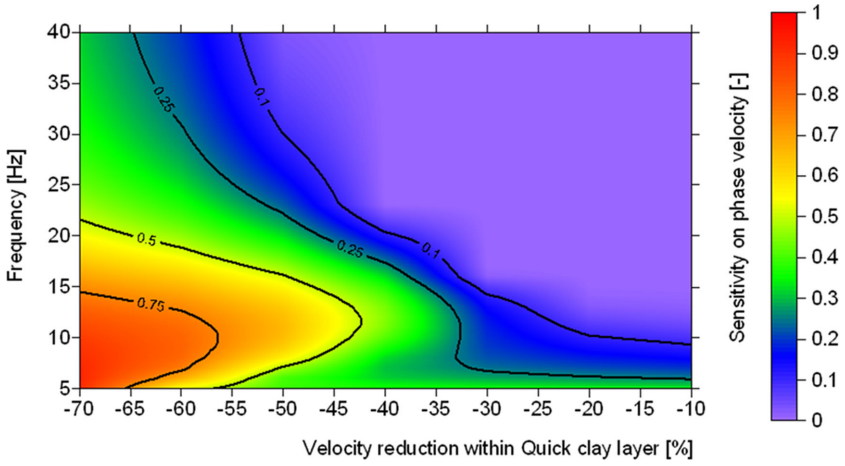

Figure 9. Phase-velocity sensitivity in the frequency band observed in the field data with respect to a velocity reduction in the quick-clay layer.

obtained from the dispersion curve inversion that was not possible to derive from reflection seismic velocity analysis at comparable depths (Fig. 3b).

The application of a moving Gaussian window along the seismic line allowed a high lateral resolution to be obtained, thus providing a detailed mapping of the lvl associated to quick clay and of other relevant geological formations. The key point of this approach is the balance required between lateral resolution and wavenumber resolution. Indeed, the more local the dispersion curves (i.e. the greater the lateral resolution), the more accurately lateral variations can potentially be reconstructed (Bergamo *et al.* 2012). However, wavenumber resolution of the *f–k* spectra gets poorer if too narrow windows are used and, consequently, the extracted curve quality is compromised.

In order to evaluate possible influence of higher modes in the dispersion curve a multimodal modeling test was conducted. As a benchmark, the 1-D inverted stratigraphy obtained by LCI from the dispersion curve nearest to the direct sounding (i.e. 150 m offset) was used (Fig. 8c). This modeling also aimed at further assessing the sensitivity to the lvl in the dispersion curve extracted through the Gaussian window. Results of the multimodal modeling are reported in Fig. 8 and compared with field data. It is evident that in the modeled data, the modal curves show a peculiar pattern with fundamental and first higher modes sharing a point that is typical of the presence of velocity inversions within the layered system. This is reflected in a marked curvature of the fundamental mode around 20 Hz, and in a partial superposition with the first higher mode (Fig. 8b). This behaviour is correctly picked in experimental data by means of the Gaussian windowing approach.

The outlined lvl was present in the initial model (layer 3) of the LCI and attempts in imaging the velocity inversion with different starting models were not successful, hence the reliability of this information should be further assessed. To evaluate the reliability of Love-wave dispersion data, a sensitivity analysis has been conducted on the same stratigraphy reported in Fig. 8(c), by changing the velocity of the third layer and evaluating the effect of these changes in the dispersion curve pattern. Dispersion curve sensitivity for different amounts of velocity reduction within quick-clay layer, with respect to above non-leached clays, is presented in Fig. 9. Sensitivity is reported, in the frequency band observed in experimental data, in terms of normalized phase-velocity variation with respect to a

uniform velocity model. This means that a 0.25 sensitivity in a particular frequency range will result in a 25 per cent variation of phase velocities in that range, due to the presence of the lvl at depth.

Results of the sensitivity analysis show that from *ca.* 30 per cent velocity reduction in the quick-clay layer an experimentally detectable difference in phase velocity can be observed (sensitivity above 0.25). For the present case study, the most significant phase-velocities variations (colours from green to red in Fig. 9) occur around 20 Hz which is where the fundamental and the higher modes are coincident. The sensitivity to the lvl in the stratigraphy increases from *ca.* 30 per cent velocity reduction on (about 0.5 at 60 per cent velocity reduction), reflecting the increased reliability in the identification of stronger velocity contrasts. The threshold frequency band at which the increase in sensitivity is more relevant depends on the depth of the lvl which is intended to be imaged and is strictly related to the penetration depth of surface waves.

The amount of velocity decreases in the layer corresponding to quick clay in the LCI final section, and in the model reported in Fig. 7(b), is comparable to literature data about the effect of leaching on clay materials. Sauvin *et al*. (2013) reported shear wave velocity values in the range of 80–150 m s^{-1} for leached clays. Bjerrum (1954) showed that leaching could cause a shear strength reduction in the order of 40 per cent from the original material and, by collecting different Norwegian clay samples, observed relatively constant density values which showed no particular correlation with material sensitivity. Depending on the proposed correlations (Dickenson 1994; Andersen 2004; Taboada *et al.* 2013; NGI 2015; L'Heureux & Long 2017) between *Vs* and undrained shear strength different ranges of reduction could be attended in the shear wave velocity from non-leached clay to quick clays.

6 CONCLUSIONS

We have shown that the analysis of Love-wave dispersion curves is useful to derive fine-tuned lateral and vertical shear wave velocity variability. The dispersion curves are extracted from seismic reflection data with Gaussian windowing and inverted with a LCI including structural *a priori* information from seismic reflection imaging. A weak velocity inversion was observed in some of the shear wave velocity profiles along the line and can be related to highly sensitive material.

Even though the available dispersion data were band limited, since targeted to high-resolution reflection imaging, and the *S*-wave properties of quick clays need to be further investigated, the results of this field experiment represent a promising confirmation of the potential of the proposed approach for imaging the shear wave velocity distribution. With respect to quick-clay identification, shear wave velocity arises as a valuable diagnostic parameter alternative to other geophysical methods (e.g. resistivity).

A priori information from seismic reflection provided a useful constraint for accurate mapping of lvls. This was necessary because limited contrast of shear wave velocity with respect to the background can cause that the sensitivity of dispersion curves regarding lvls is not always sufficient for a reliable inversion. Further investigations are still required in order to fully understand this information. However, the procedure described here yields high potential of dispersion data for the mapping of quick clay or other low-velocity sequences in the subsurface.

Particularly, the proposed Gaussian windowing approach and LCI have shown their potentiality in evidencing lateral variations even in very challenging situations like the ones of the present case study. A wider application of the methodology to similar targets, or for understanding both marine and terrestrial landslide processes in general, will result in a more comprehensive imaging of *Vs* properties useful for different applications in applied and geodynamic research.

The use of dispersion data should be targeted to the required investigation depth. It is particularly important to acquire a broad frequency band to allow for a proper low-frequency picking of the dispersion data to overcome limitations in the investigation depth. Thereby, not only local geophysical characterization would be achieved but also the determination of site effects leading to a better constrained hazard and risk assessment could be enabled.

ACKNOWLEDGEMENTS

The work presented here was partly funded by the Society of Exploration Geophysicists within its Geoscientists Without Borders programme (data acquisition). The other part came through the DAAD exchange programme which funded the research scholarship of one of the authors for a stay at Leibniz-Institut für Angewandte Geophysik.

REFERENCES

Andersen, K.H., 2004. Cyclic clay data for foundation design of structures subjected to wave loading, in *Cyclic Behaviour of Soils and Liquefaction Phenomena, Proceedings of the International Conference*, 31 March–2 April 2004, Th. Triantafyllidis, pp. 371–387, Taylor & Francis, Bochum, Germany.

Auken, E. & Christiansen, A.V., 2004. Layered and laterally constrained 2D inversion of resistivity data, *Geophysics,* **69,** 752–761.

Bergamo, P., Boiero, D. & Socco, L.V., 2012. Retrieving 2D structures from surface-wave data by means of space-varying spatial windowing, *Geophysics,* **77**(4), EN39–EN51.

Bjerrum, L., 1954. Geotechnical properties of Norwegian marine clays, *Geotechnique,* **4,** 49–69.

Choquette, M., Bérubé, M.-A. & Locat, J., 1987. Mineralogical and microtextural changes associated with lime stabilization of marine clays from eastern Canada, *Appl. Clay Sci.,* **2**(3), 215–232.

Crawford, C.B., 1968. Quick clays of eastern Canada, *Eng. Geol.,* **2** (4), 239–265.

Dahlin, T., Löfroth, H., Schälin, D. & Seur, P., 2013. Mapping of quick clay using geoelectrical imaging and CPTU-resistivity, *Near Surf. Geophys.,* **11,** 659–670.

Dickenson, S.E., 1994. Dynamic response of soft and deep cohesive soils during the Loma Prieta Earthquake of October 17, 1989, *PhD thesis*, Department of Civil and Environment Engineering, University of California, Berkeley, CA.

Donohue, S., Long, M., O'Connor, P., Helle, T.E., Pfaffhuber, A.A. & Rømoen, M., 2012. Multi-method geophysical mapping of quick-clay, *Near Surf. Geophys.,* **10,** 207–219.

Fabien-Ouellet, G., Fortier, R. & Giroux, B., 2014. Joint acquisition and processing of seismic reflections and surface waves in a sensitive clay deposit in the Outaouais Region (Québec), Canada, in *Landslides in Sensitive Clays*, Vol. 36, pp. 241–252, Springer, The Netherlands.

Geertsema, M., Clague, J.J., Schwab, J.W. & Evans, S.G., 2006. An overview of recent large catastrophic landslides in northern British Columbia, Canada, *Eng. Geol.,* **83**(1–3), 120–143.

Krawczyk, C.M., Polom, U., Trabs, S. & Dahm, T., 2012. Sinkholes in the city of Hamburg—new urban shear-wave reflection seismic system enables high-resolution imaging of subrosion structures, *J. appl. Geophys.,* **78,** 133–143.

Krawczyk, C.M., Polom, U., Malehmir, A. & Bastani, M., 2013a. Quick-clay landslides in Sweden: insights from shear-wave reflection

seismics and geotechnical integration, in *Proceedings of the Near Surface Geoscience 2013*, Bochum/Germany, doi:10.3997/2214-4609.20131348, p. 5.

Krawczyk, C.M., Polom, U. & Beilecke, T., 2013b. Shear-wave reflection seismics as valuable tool for near-surface urban applications, *Leading Edge,* **32**(3), 256–263.

L'Heureux, J.-S. & Long, M., 2017. Relationship between shear-wave velocity and geotechnical parameters for Norwegian clays, *J. Geotech. Geoenviron. Eng.*, **143**(6), doi:10.1061/(ASCE)GT.1943-5606.0001645.

Löfroth, H., Suer, P., Dahlin, T., Leroux, V. & Schälin, D., 2011. Quick-clay mapping by resistivity—surface resistivity, CPTU-R and chemistry to complement other geotechnical sounding and sampling, Report No. 30, Swedish Geotechnical Institute, Linköping.

Lundström, K., Larsson, R. & Dahlin, T., 2009. Mapping of quick-clay formations using geotechnical and geophysical methods, *Landslides,* **6,** 1–15.

Malehmir, A., Bastani, M., Krawczyk, C.M., Gurk, M., Ismail, N., Polom, U. & Person, L., 2013. Geophysical assessment and geotechnical investigation of quick-clay landslides—a Swedish case study, *Near Surf. Geophys.,* **11,** 341–350.

Nadim, F., Pedersen, S.A.S., Schmidt-Thomé, P., Sigmundsson, F. & Engdahl, M., 2008. Natural hazards in Nordic countries, *Episodes,* **31,** 176–184.

NGI (Norwegian Geotechnical Institute), 2015. Correlations between shear wave velocity and geotechnical parameters in Norwegian clays, Report SP8-GEODIP.

Osterman, J., 1964. Studies on the properties and formation of quick clays, claus and clay minerals, Monograph No. 19, Earth Science Series, Pergamon Press, pp. 87–108.

Polom, U., Arsyad, I. & Kuempel, H.-J., 2008. Shallow shear-wave reflection seismics in the tsunami struck Krueng Aceh River Basin, Sumatra, *Adv. Geosci.,* **14,** 135–140.

Polom, U., Hansen, L., Sauvin, G., L'Heureux, J.-S., Lecomte, I., Krawczyk, C.M., Vanneste, M. & Longva, O., 2010. High-resolution SH-wave reflection seismics for characterization of onshore ground conditions in the Trondheim harbor, central Norway, in *Advances in Near-Surface Seismology and Ground-Penetrating Radar*, pp. 297–312, eds Miller, R.D., Bradford, J.D. & Holliger, K., SEG, Tulsa.

Polom, U., Bagge, M., Wadas, S., Winsemann, J., Brandes, C., Binot, F. & Krawczyk, C.M., 2013. Surveying near-surface depocentres by means of shear wave seismics, *First Break,* **31**(8), 67–79.

Rankka, K., Andersson-Sköld, Y., Hultén, C., Larsson, R., Leroux, V. & Dahlin, T., 2004. Quick-clay in Sweden, Report No. 65, Swedish Geotechnical Institute, Linköping.

Salas-Romero, S., Malehmir, A., Snowball, I., Lougheed, B.C. & Hellqvist, M., 2016. Identifying landslide preconditions in Swedish quick clays – insights from integration of surface geophysical, core sample- and downhole property measurements, *Landslides,* **13**(5), 905–923.

Sauvin, G., Lecomte, I., Bazin, S., L'Heureux, J.-S., Vanneste, M., Solberg, I.-L. & Dalsegg, E., 2013. Towards geophysical and geotechnical integration for quick-clay mapping in Norway, *Near Surf. Geophys.,* **11**(6), 613–623.

SGI, 2012. Strength degradation of clay due to cyclic loadings and enforced deformation, Report 75, SE-581 93, Linköping.

Socco, L.V., Boiero, D., Foti, S. & Wisén, R., 2009. Laterally constrained inversion of ground roll from seismic reflection records, *Geophysics,* **74**(6), G35–G45.

Söderblom, R., 1969. *Salt in Swedish Clays and its Importance for Quick-clay Formation. Results from Some Field and Laboratory Studies*, Vol. 22, Swedish Geotechnical Institute, Stockholm.

Solberg, I.-L., Rønning, J.S., Dalsegg, E., Hansen, L., Rokoengen, K. & Sandven, R., 2008. Resistivity measurements as a tool for outlining quick-clay extent and valley-fill stratigraphy: a feasibility study from Buvika, central Norway, *Canadian Geotech. J.,* **45,** 210–225,

Solberg, I.L., Hansen, L., Ronning, J.S., Haugen, E.D., Dalsegg, E. & Tonnesen, J.F., 2012. Combined geophysical and geotechnical approach to ground investigations and hazard zonation of a quick-clay area, mid Norway, *Bull. Eng. Geol. Environ.,* **71,** 119–133.

Taboada, V.M., Cruz, D. & Barrera, P., 2013. *Predictive Equations of Shear Wave Velocity for Bay of Campeche Clay, Offshore Technology Conference (OTC),* Vol. OTC 24068, Heuston, Texas, OTC.

Torrance, J.K., 1983. Towards a general model of quick-clay development, *Sedimentology,* **30,** 547–555.

Wisén, R. & Christiansen, A.V., 2005. Laterally and mutually constrained inversion of surface wave seismic data and resistivity data, *J. Environ. Eng. Geophys.,* **10**(3), 251–262.